How does the flagellum affect the swimming of bacteria?

Magali Tournus

Mathematics Department - Penn State University
CSCAMM - University of Maryland

Collaborators : Igor Aronson, Leonid Berlyand and Arkadz Kirshtein

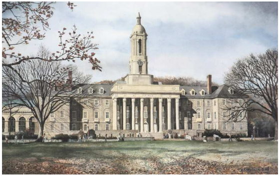

1. Motivation

2. Description of the model

3. Trarjectory of the swimmer
    - Previous results
    - In a Planar Shear Flow : Asymptotic analysis
    - In a Poiseuille flow : Numerical result

4. Conclusions and future work

Motivation for studying a suspension of self-propelled micro-swimmers

Current questions of interest about micro-swimmers:

Microscopic scale : How do they swim? What determines their trajectory? Can we control them?

Macroscopic scale : Collective motion? Pattern formation? Property of the complex fluid made by the suspension?

Examples of self-propelled flagellated micro-swimmers

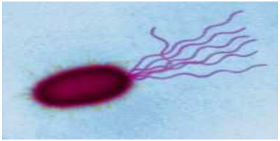

Escherichia Coli

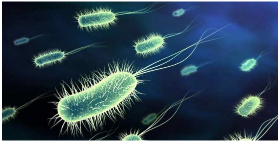

Bacilus Subtilis

Experimental observation

The **Effective Viscosity** *of a fluid containing self-propelled swimming bacteria is smaller, compared to the* **Effective Viscosity** *of a fluid containing dead bacteria.*

Why is it important? Small viscosity ≈ Better motility of macroscopic objects

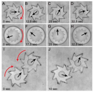

Ingredients needed in models predicting decrease of Effective viscosity :
Self-propulsion + Elongated body + Random tumbling (Haines et al., 2009)
Self-propulsion + Elongated body + Hydrodynamic interactions + pair-wise interactions (Ryan et al., 2013)

However : A viscosity reduction has been measured without noticeable tumbling (Sokolov/Aronson et al. (2007,09)) for dilute suspensions of Bacillus Subtilis.

A model which predicts the decrease of viscosity in dilute suspension without tumbling is needed.

The flagellum as a key ingredient in the viscosity decrease

A bacterium is composed of a body + several flagella distributed over the surface of its body, which allow the bacterium to swim (forward movement).

Until now, at the microscopic level, swimmers are modeled as **rigid ellipsoid** with a propulsion force concentrated somewhere behind the body.

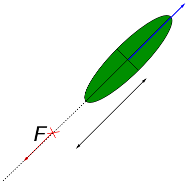

One hypothesis is that **the geometry and physical properties of the flagellum may affect the trajectories, and thus the rheological properties** of a bacterial suspension.

To **check this hypothesis**, we develop a more accurate model of the flexible flagellum, and see how it affects the evolution of trajectories and orientation of the bacterium.

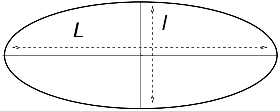

$$a = \frac{L^2}{l^2 + L^2}, \quad b = \frac{l^2}{l^2 + L^2}$$

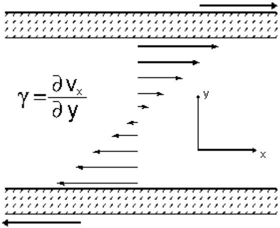

Jeffery Equation:

$$\begin{cases} \dfrac{d\theta(t)}{dt} = \gamma\left[a\sin^2\theta(t) + b\cos^2\theta(t)\right], \\ \theta(0) = 0. \end{cases}$$

Solution:

$$\theta(t) = \text{Arctan}\left(\frac{b}{\sqrt{ab}}\tan(\sqrt{ab}t)\right)$$

Fast rotation when perpendicular to the flow
Slow rotation when parallel to the flow

- Flagellated organisms such as bacteria utilize the fluid drag anisotropy of flagella in order to propel themselves through a viscous fluid.

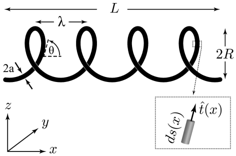

- Bacteria such as B. subtilis actuate passive helical filaments using rotary motors embedded in the cell walls, and whose rotation gives rise to propulsion (as a propeller).
  The force exerted by the flagellum propell the swimmer which moves forward (pushers) or backward (pullers) and modifies the velocity flow around the swimmer, which slows down the swimmer (drag force).

- The motor is driven by protons flowing from the outside to the inside of the cell creating a transmembrane electrical potential.
  CW and CCW modes alternate.
  When the motors turn CW, the flagellar filaments work independently, and the cell body moves erratically : tumble. When the motors turn CCW, the filaments rotate in parallel in a bundle that pushes the cell body steadily forward : run.

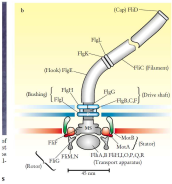

Different models of flagellated swimmers for different purposes (Non exhaustive history)

- For the issue of viscosity in shear flows or mixing enhancement: Ellipsoid, with a point force directed radially outward from the body Hatwalne (04), Haines/Berlyand/Aranson (08), Riffer/Zimmel (07), Decoene (10).

- For the issue of collective behavior : Self locomoting rod Saintillan (07). Force dipole model, with size and shape, Ryan/Berlyand/Sokolov/Aranson (12), Dresher (11) .

- For understanding the dynamics of a bacterium in a fluid :
  - Idealized sphere in a streaming fluid Bretherton/ Rotchild (61), Kessler (85).
  - Relationship between angular and translational velocities and force for an helix model Purcell (97), extended to superhelices by Jung et al (07).
  - Introduction of a precise model of the helical flagellum to adress the question on the effect of chiral forces on the dynamic in a shear flow Marcos (11) .
  - Elastic plate equation to model the elastic flagellum : Hines/Blum (78), Stone (06)

Description of the model

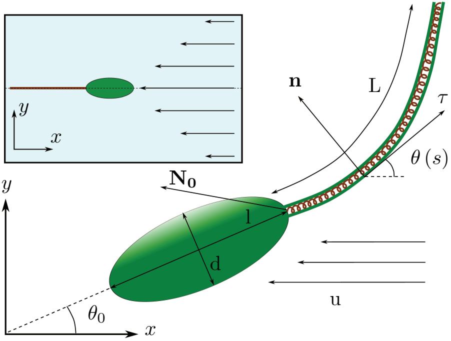

The 2D swimmer is composed of a rigid body, rigidly attached to a flexible flagellum.
The swimmer in plunged in a given flow u.

Along the flagellum is generated a force of total intensity F, that is transmitted to the body, and which is responsible for the swimmer propulsion.

The flagellum

- Balance of force [Physical framework : Resistive force theory]

$$\frac{\partial}{\partial s}\Big(\Lambda\tau + N\mathbf{n}\Big) = \zeta_f\Big(v_\tau - u(y)\cos\theta\Big)\tau + \alpha\zeta_f\Big(v_n + u(y)\sin\theta\Big)\mathbf{n} - F\tau.$$

- Balance of torque [Physical hypothesis : Flagellum is inextensible]

$$N(s) = -K_b\frac{\partial^2\theta}{\partial s^2}(s).$$

- Boundary conditions [Physical hypothesis : The flagellum end is free]

$$\frac{\partial\theta}{\partial s}(L,\ t) = \frac{\partial^2\theta}{\partial s^2}(L,\ t) = \Lambda(L,\ t) = 0,$$

The body : [Physical hypothesis : The body is rigid]

$$\frac{d\theta_0}{dt} = -\dot{\gamma}\left(\frac{l^2}{l^2+d^2}\sin^2\theta_0 + \frac{d^2}{l^2+d^2}\cos^2\theta_0\right) + \frac{l}{2\zeta_r}N_0,$$

Interface conditions : [Physical hypothesis : Attachment is rigid]

$$\theta(0,\ t) = \theta_0(t), \quad \Lambda(0,\ t) = \Lambda_0(t),$$

$$v_\tau(0) = v_{\tau,0}, \qquad v_n(0) = v_{n,0} + \frac{l}{2}\frac{d\theta_0}{dt}.$$

- **Parameter**: $\beta = \dfrac{l^2}{l^2 + d^2}$.

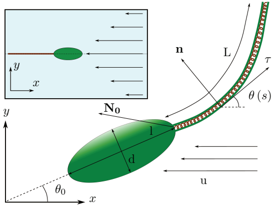

- **Variables**:
  Head angle : $\theta_0(t)$
  Head y-component: $y_0(t)$

- **The equations**:

$$\begin{cases} \dfrac{d\theta_0}{dt}(t) = -u'(y_0(t))\Big((1-\beta)\sin^2\theta_0(t) + \beta\cos^2\theta_0(t)\Big) + \dfrac{3L}{l} k_r N_0(t), \\ \dfrac{dy_0}{dt}(t) = k_r \Lambda_0(t)\sin(\theta_0(t)) + \dfrac{k_r}{\alpha} N_0(t)\cos(\theta_0(t)), \\ \quad y_0(0) = y_{0,in}, \quad \theta_0(0) = \theta_{0,in}. \end{cases}$$

- **Parameters** :
  Bending stiffness K_b
  Propulsion force F

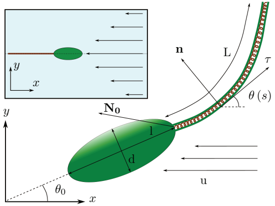

- **Variables**:
  Angle of the flagellum : $\theta(s, t)$
  Tangential intenal stress : $\Lambda(s, t)$

- **The equations** : Angle

$$\left\{ \begin{array}{l} \frac{\partial \theta}{\partial t} = -\frac{K_b}{\alpha}\frac{\partial^4 \theta}{\partial s^4} + (\frac{1}{\alpha}\Lambda + K_b(\frac{\partial \theta}{\partial s})^2)\frac{\partial^2 \theta}{\partial s^2} + (\frac{\alpha+1}{\alpha}\frac{\partial \Lambda}{\partial s} + F_p)\frac{\partial \theta}{\partial s} - u'(y)\sin(\theta)^2, \\ \frac{\partial \theta}{\partial s}(1,\ t) = \frac{\partial^2 \theta}{\partial s^2}(1,\ t) = 0, \\ \theta(0,\ t) = \theta_0(t), \quad -K_b\frac{\partial^2 \theta}{\partial s^2}(0,\ t) = N_0(t) \end{array} \right.$$

Tangential intenal stress

$$\left\{ \begin{array}{l} \frac{\partial^2 \Lambda}{\partial s^2} = \frac{1}{\alpha}\Lambda(\frac{\partial \theta}{\partial s})^2 - K_b(\frac{\partial^2 \theta}{\partial s^2})^2 - u'(y)\sin(\theta)\cos(\theta) - \frac{(\alpha+1)}{\alpha}K_b\frac{\partial^3 \theta}{\partial s^3}\frac{\partial \theta}{\partial s}, \\ \Lambda(1,\ t) = 0, \quad \Lambda(0,\ t) = \Lambda_0(t) \end{array} \right.$$

- **Parameters** :
  Bending stiffness K_b
  Propulsion force F

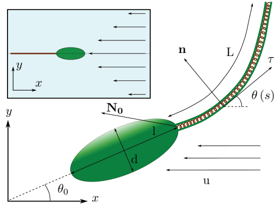

- **Variables**:
  Tangential intenal stress : $\Lambda_0(t)$
  Normal intenal stress : $N_0(t)$

- **The equations** (Velocity equality) :
  Tangential component :

$$k_r\Lambda_0 = \frac{\alpha}{L}\Big(u(y(0)) - u(y^h)\Big)\cos(\theta_0) + \frac{\partial \Lambda}{\partial s} + F - \frac{\partial \theta}{\partial s}N_0, \qquad s = 0, \tag{1}$$

Normal component :

$$\left(\frac{\alpha}{\alpha_h} + \frac{3\alpha}{2}\right)k_r N_0 = -\frac{\alpha}{L}\sin(\theta_0)\Big(u(y(0)) - u(y^h)\Big) + \frac{\alpha l}{2L}u'(y)\Big[(1-\beta)sin^2(\theta_0) + \beta cos^2(\theta_0)\Big]$$
$$+\Big[-K_b\frac{\partial^3\theta}{\partial s} + \frac{\partial \theta}{\partial s}\Lambda\Big], \qquad s = 0, \tag{2}$$

Dynamic of the swimmer in a planar shear flow

Planar shear flow $u(y) = \gamma y$

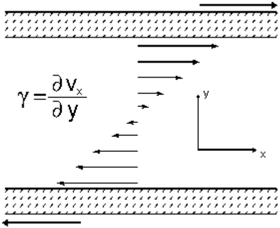

What we want to capture

1. The time evolution of the swimmer orientation $\theta_0(t)$, compared to the orientation given by Jeffery orbit.

$$\frac{d\theta_0}{dt}(t) = -\gamma\Big((1-\beta)\sin^2\theta_0(t) + \beta\cos^2\theta_0(t)\Big) + \frac{3L}{l} k_r N_0(t),$$

2. The shape of the flagellum.

Identification of the behavior for large K_b (rigid flagellum)

- We write the asymptotic expansions

$$\begin{cases} \theta(s,t) = \theta^0(s,t) + \frac{1}{K_b}\theta^1(s,t), \qquad \theta_0(t) = \theta_0^0(t) + \frac{1}{K_b}\theta_0^1(t), \\ \Lambda(s,t) = \Lambda^0(s,t) + \frac{1}{K_b}\Lambda^1(s,t), \qquad \Lambda_0(t) = \Lambda_0^0(t) + \frac{1}{K_b}\Lambda_0^1(t), \\ N_0(t) = N_0^0(t) + \frac{1}{K_b}N_0^1(t), \end{cases}$$

- Plug into the non-linear system, identify the term of same order to get an equation on θ_0^0.
- To refine the result, compute the corrector θ_0^1.

  Resonance appears : the asymptotic expansion does not converge.

Identification of the behavior for large K_b (rigid flagellum).

- Introduce a small time scale $\tau = \frac{t}{K_b}$.
- Write the asymptotic expansions

$$\begin{cases} \theta(s,t,\tau) = \theta^0(s,t,\tau) + \frac{1}{K_b}\theta^1(s,t,\tau), & \theta_0(t,\tau) = \theta_0^0(t,\tau) + \frac{1}{K_b}\theta_0^1(t,\tau), \\ \Lambda(s,t,\tau) = \Lambda^0(s,t,\tau) + \frac{1}{K_b}\Lambda^1(s,t,\tau), & \Lambda_0(t,\tau) = \Lambda_0^0(t,\tau) + \frac{1}{K_b}\Lambda_0^1(t,\tau), \\ N_0(t,\tau) = N_0^0(t,\tau) + \frac{1}{K_b}N_0^1(t,\tau), & \end{cases}$$

- By identifying the terms of order **0**, we obtain the modified Jeffery's equation:

$$\begin{cases} \frac{\partial \theta_0^0(t,\tau)}{\partial t} = A \sin^2 \theta_0^0(t,\tau) + B \cos^2 \theta_0^0(t,\tau), \\ \theta(0,\tau) = ?, \qquad \text{Given by order 1}. \end{cases}$$

with A and B determined by the geometrical and physical parameters of the model.

Asymptotic analysis - Two-time scale method

The equation on the corrector $\boldsymbol{\theta_0^1}$ is

$$\left(\frac{\partial\theta_0^0}{\partial\tau} + \frac{\partial\boldsymbol{\theta_0^1}}{\partial t}\right) = C\boldsymbol{\theta_0^1}\sin(2\theta_0^0) + C_1\sin(2\theta_0^0) + C_2\sin(2\theta_0^0)\cos(2\theta_0^0) + C_sF\cos(2\theta_0^0),$$

where C_1, C_2 and $C_s < 0$ are constants depending on the geometrical parameters.

Secular term : $C_sF\cos(2\theta_0^0)$.

To prevent any resonance to appear, we impose :

$$\frac{\partial\theta_0^0}{\partial\tau} = C_sFxdf\cos(2\theta_0^0(t,\tau)).$$

The equations for order 0 thus are :

$$\begin{cases} \dfrac{\partial\theta_0^0}{\partial t}(t,\tau) = A\sin^2\theta_0^0(t,\tau) + B\cos^2\theta_0^0(t,\tau), \\ \dfrac{\partial\theta_0^0}{\partial\tau}(t,\tau) = C_sF\cos(2\theta_0^0(t,\tau)), \\ \theta_0^0(0,0) = 0. \end{cases}$$

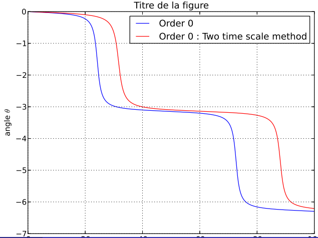

Modified Jeffery equation :

$$\frac{d\theta_0^0}{dt} = -(1-b)\sin^2\theta_0 - b\cos^2\theta_0$$

In the limit $K_b = +\infty$ the evolution of the bacterial body angle is given asymptotically by

$$\theta_0^0(t) = \arctan\left[\sqrt{\frac{b}{1-b}}\tan\left(\sqrt{(1-b)b}\,t\left(1-\frac{c}{K_b b}\right)\right)\right],$$

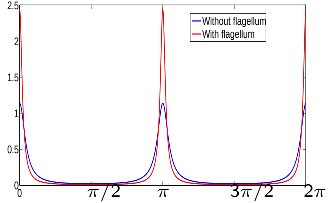

where $\quad b \leq \beta \quad 1-b \geq 1-\beta, \quad c < 0.$

As $\beta < \frac{1}{2}$, it means that

- In regions where the ellipsoidal body rotates fast, the flagellum makes it rotate faster,
- In regions where the ellipsoidal body rotates slow, the flagellum makes it rotate slower.

Proposition

In a **planar shear flow**, *the* **trajectories of flagellated swimmers are periodic**. *The period is determined by the elasticity of the flagellum:* **the softer the flagellum, the smaller the period**.

About the numerical scheme :

It is shown to be **robust**, **convergent**, and **gives the right solution on simple basal cases**.

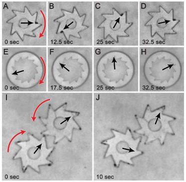

Shape of the swimmer for different body orientations :

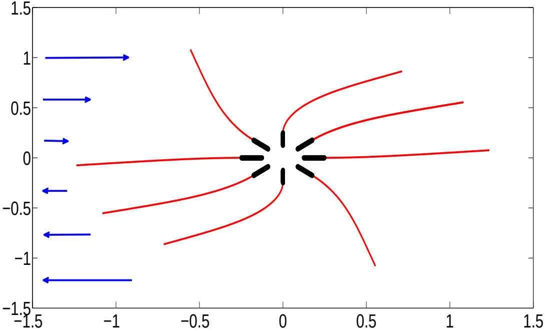

The flagellum is shaped by the flow (prevails for $\theta_0 = \frac{\pi}{2}$) and by the body rotation (prevails for $\theta_0 = 0$),

Dynamic of the swimmer in a Poiseuille flow

Rigid self-propelled ellipsoid plunged in a Poiseuille flow.
y-coordinate of the body : $y_0(t)$, angle of the body $\theta_0(t)$

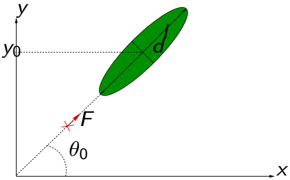

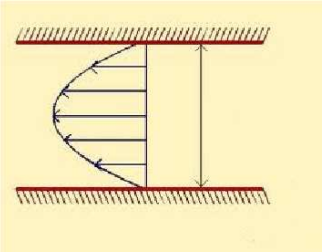

$$\begin{cases} \dfrac{dy_0(t)}{dt} = -F\sin(\theta_0(t)), \quad y_0(0) = y_{c,0}, \\ \dfrac{d\theta_0(t)}{dt} = -2py_0(t)\Big((1-\beta)\sin^2\theta_0(t) + \beta\cos^2\theta_0(t)\Big), \quad \theta_0(0) = \theta_0^0. \end{cases}$$

Result of Zottl-Stark : **Trajectories are periodic**.

The structure of the dynamic

$$\begin{cases} \dfrac{dy^c(t)}{dt} = k_r \Lambda_0(t) \sin(\theta_0(t)) + \dfrac{k_r}{\alpha_h} N_0(t) \cos(\theta_0(t)), \quad y^c(0) = y_0^c, \\ \dfrac{d\theta_0(t)}{dt} = -2py^c(t)\Big((1-\beta)\sin^2\theta_0(t) + \beta\cos^2\theta_0(t)\Big) + \dfrac{3L}{l} k_r N_0(t), \end{cases}$$

where N_0 is given by solving

$$B_{K_b}(N_0, \theta_0, y^c) = 0.$$

- $N_0 = 0$: No flagellum - *Previous result*
- $B_{+\infty}(N_0, y^c, \theta_0) = 0 \to N_0 = B^{-1}(y^c, \theta_0)$: Rigid flagellum - *Asymptotic analysis*
- $B_{K_b}(N_0, y_c, \theta_0) = 0$: General case - *Numerical analysis*

Movie

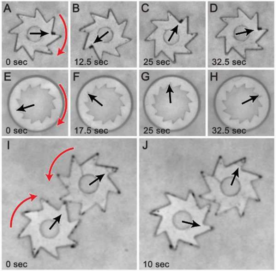
A
0 sec
B
12.5 sec
C
25 sec
D
32.5 sec
E
0 sec
F
17.5 sec
G
25 sec
H
32.5 sec
I
0 sec
J
10 sec

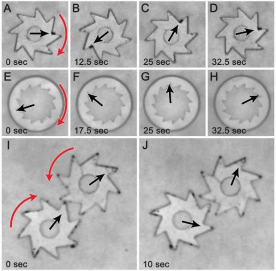
A
0 sec
B
12.5 sec
C
25 sec
D
32.5 sec
E
0 sec
F
17.5 sec
G
25 sec
H
32.5 sec
I
0 sec
J
10 sec

Trajectory in Poiseuille flow for large K_b - Numerics

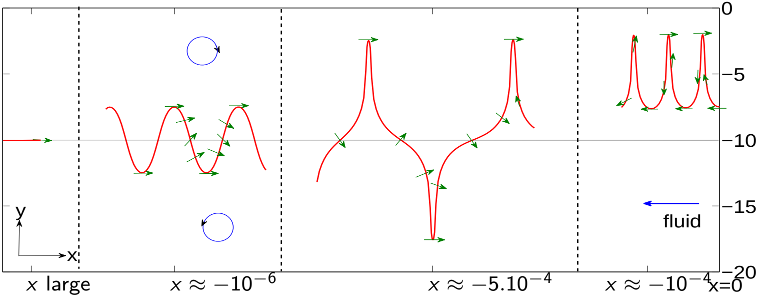

Numerical Observation

In large time, the swimmer converges to the centerline of the channel and orients against the flow.

Proposition

The state $[y = 0,\ \theta = \pi]$ *is linearly stable, whereas* $[y = 0,\ \theta = 0]$ *is not.*

The linearized system around the stationary state $[y = 0,\ \theta = \pi]$:

$$\begin{cases} \dfrac{d\theta_0(t)}{dt} = -2py(t) + 3N_0(t), \\ \dfrac{dy(t)}{dt} = \dfrac{F_p \cos(\pi)}{3}\theta_0(t) + \dfrac{\cos(\pi)}{4}N_0(t), \end{cases}$$

where N_0 is asymptotically determined by

$$N_0 = -\frac{1}{3}\Big(\frac{d\theta_0}{dt} + \beta py\Big).$$

$$A = \begin{pmatrix} 0 & -2p \\ \dfrac{F_p \cos(\pi)}{3} & 0 \end{pmatrix}$$

Heuristics (large K_b) - Why does the swimmer reaches the center

Two mechanisms are responsible for the convergence toward the center

- **The rigidity of the flagellum tends move the center of mass of the swimmer,**

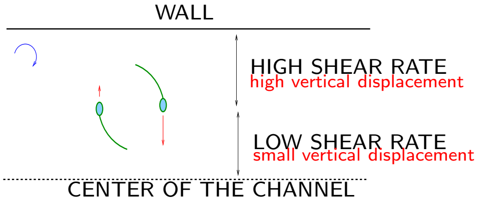

- **The propulsion force amplifies this phenomenon**

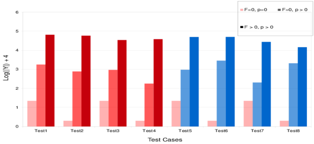

Non-monotonic behaviour depending on the bending stiffness

Numerical Observation

For $K_b = 20$ (realistic value for B.Subtilis is $K_b = 30$) the self-propelled swimmer no longer drifts toward the center, but instead converges towards a limit cycle , where the swimmer swings around the centerline.

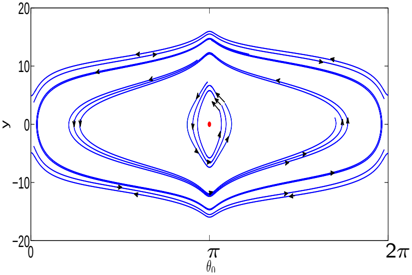

$K_b = 30$

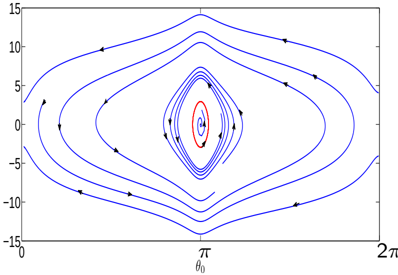

$K_b = 20$

Non-monotonic behaviour depending on the bending stiffness

Numerical Observation

For $K_b = 20$ the self-propelled swimmer no longer drifts toward the center, but instead converges towards a limit cycle , where the swimmer swings around the centerline. When further decreasing the bending stiffness ($K_b = 10$), the behavior is again similar to $K_b = 30$. This suggests that the behavior of the system is very complex and highly non trivial.

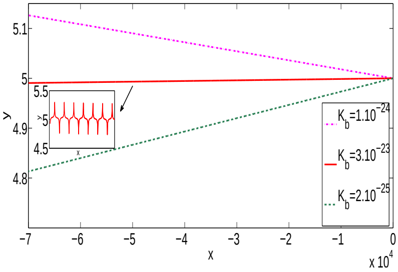

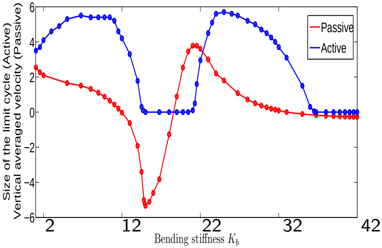

The buckling effect

The coefficient in front of the second order term has the bad sign.

$$\begin{cases} \dfrac{\partial \theta}{\partial t} = -\dfrac{K_b}{\alpha}\dfrac{\partial^4 \theta}{\partial s^4} + \left(\dfrac{1}{\alpha}\Lambda + K_b\left(\dfrac{\partial \theta}{\partial s}\right)^2\right)\dfrac{\partial^2 \theta}{\partial s^2} + \left(\dfrac{\alpha+1}{\alpha}\dfrac{\partial \Lambda}{\partial s} + F_p\right)\dfrac{\partial \theta}{\partial s} - u'(y)\sin(\theta)^2, \\ \quad \dfrac{\partial \theta}{\partial s}(1,\ t) = \dfrac{\partial^2 \theta}{\partial s^2}(1,\ t) = 0, \\ \quad \theta(0,\ t) = \theta_0(t), \quad -K_b \dfrac{\partial^2 \theta}{\partial s^2}(0,\ t) = N_0(t) \end{cases}$$

Euler Buckling of the flagellum is likely to occur.

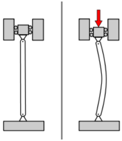

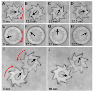

Conclusions

- **Derivation of a non-linear PDE model that couples body motion of a swimmer with bending flagellum attached to it.**

- **Linear asymptotic analysis of this model for planar shear flow shows how classical Jeffery orbits change due to the presence of the flagellum.**

- **Numerical analysis in Poiseuille : The model exhibits non periodic trajectories due to the presence of the flagellum : contrast with classical periodic trajectories for Jeffery equation**

- **Open question** : Can we understand the convergence toward the steady state/limit cylce via analysis?

- **Macroscopic properties:** How does the presence of the flagellum modifies the rheology of the bacterial suspension? (work in progress)

- **Collective motion** : How does the presence of the flagellum modifies pasive hydro-dynamic interactions?

- Derivation of kinetic models including the flagellum at the miroscopic scale?